The 9th European Congress on Computational Methods in Applied Sciences and Engineering
ECCOMAS Congress 2024
3–7 June 2024, Lisboa, Portugal

UNSTRUCTURED CONSERVATIVE LEVEL-SET METHOD FOR INTERFACIAL TRANSPORT PROCESSES ON ADAPTIVE AND FIXED COLLOCATED MESHES

N. Balcázar-Arciniega[1,*], J. Rigola[1] and A. Oliva[1]

[1,*] Heat and Mass Transfer Technological Centre (CTTC),
Universitat Politècnica de Catalunya (UPC) - BarcelonaTech,
ESEIAAT, Colom 11, 08222 Terrassa (Barcelona), Spain.
nestor.balcazar@upc.edu , nestorbalcazar@yahoo.es

Key words: Unstructured Conservative Level-Set Method, Unstructured Flux-Limiters, Finite-Volume Method, Unstructured Meshes, Interfacial heat transfer, Thermocapillarity, Adaptive mesh refinement

Summary. This paper reports advancements in the unstructured conservative level-set (UCLS) method for simulating two-phase flows with complex interfacial physics. The developed framework within the UCLS method addresses interfacial transport processes, including heat and mass transfer, variable surface tension, and liquid-vapor phase change. The transport equations are discretized using the finite-volume method on three-dimensional collocated unstructured meshes. The UCLS method is utilized for interface capturing, while a multiple marker approach prevents numerical coalescence in bubbles and droplets. The fractional-step projection method solves the pressure-velocity coupling in the momentum transport equation. Unstructured flux-limiter schemes approximate the convective term, and the central difference scheme calculates the diffusive term. Verifications and validations focus on the thermocapillary migration of droplets using fixed meshes with mixed control volumes and hexahdral adaptive unstructured collocated meshes.

1 INTRODUCTION

Interfacial transport phenomena, such as heat and mass transfer, thermocapillarity, and liquid-vapor phase changes, are prevalent in natural and industrial applications. These phenomena are critical in various engineering systems, including power and refrigeration cycles, petroleum and chemical processing, internal combustion engines, and sediment and pollutant transport in aquatic environments. In these systems, carrier fluids often transport bubbles or droplets of a dispersed phase. The design, optimization, and operation of such multiphase systems require a thorough understanding of the fundamental principles governing momentum, energy, and mass transport processes in individual bubbles and droplets and within swarms of fluid particles.

Transport phenomena in two-phase flows have traditionally been researched using experimental methods, often limited by optical access constraints, and theoretical methods that provide analytical solutions [27] based on simplified mathematical models. However, with the increasing computational power of supercomputers, numerical and computational methods have been empowered [49, 63]. In this sense, various techniques have been developed for Direct Numerical Simulation (DNS) of two-phase flows, classified according to the advection scheme used to track the fluid interface. Notable examples include the Volume of Fluid (VoF) method [36, 63, 49], the level-set (LS) method [48, 57], the coupled VoF-LS method [56, 55, 9], the conservative level-set (CLS) method [47, 7, 13, 19, 21], and the front-tracking

(FT) method [62]. While these methods share a common conceptual foundation, their numerical implementations on structured or unstructured meshes can differ significantly [13, 9, 8, 7].

Further efforts have extended DNS methods for complex interfacial physics. For instance, concerning two-phase flows with variable surface tension, [11, 15, 17] introduced the UCLS method for thermocapillary migration of droplets, [45, 44] reported DNS of thermocapillary migration of droplets using the FT method, [42] has performed DNS of thermal Marangoni migration using the VoF method, [25] researched thermocapillary motion of fluid particles using the LS method. On the other hand, numerical methods for liquid-vapour phase change have been extended for VoF [64, 65, 43], LS [54, 53], hybrid LS and ghost fluid [34, 60], FT [37, 32, 31, 50], unstructured CLS [12, 18], coupled VoF-LS [46, 61, 40]. Furthermore, extensions of interface capturing methods to interfacial mass transfer are reported for single bubbles [29, 23, 22, 28, 13, 21] and bubble swarms [1, 52, 39, 13, 4, 19, 13, 16, 21].

Most proposed methods for interface capturing are designed on structured and Cartesian meshes. Therefore, further efforts must be made to develop numerical methods for two-phase flow with complex interfacial physics on fixed and adaptive unstructured meshes. This work reports systematic advances in the development of numerical methods for two-phase flow with interfacial heat and mass transfer in the framework of the UCLS method proposed by Balcazar et al. [13, 11, 7, 13, 16, 21], on fixed and adaptive collocated unstructured meshes. This paper is organized as follows: Section 2 presents the mathematical formulation and the numerical methods. Verifications, validations and numerical experiments are presented in Section 3. Conclusions are reported in Section 4.

2 MATHEMATICAL FORMULATION AND NUMERICAL METHODS

2.1 Incompressible two-phase flow

The one-fluid formulation [63, 49] for incompressible two phase flow is written as follows:

$$\frac{\partial}{\partial t}(\rho \mathbf{v}) + \nabla \cdot (\rho \mathbf{v}\mathbf{v}) = -\nabla p + \nabla \cdot (\mu (\nabla \mathbf{v})) + \nabla \cdot \left(\mu (\nabla \mathbf{v})^T\right) + (\rho - \rho_0)\mathbf{g} + \mathbf{f}_\sigma, \tag{1}$$

$$\nabla \cdot \mathbf{v} = 0, \tag{2}$$

where $\mathbf{v}$ is the velocity field, p is the pressure, ρ is the fluid density, μ is the dynamic viscosity, $\mathbf{g}$ is the gravitational acceleration, $\mathbf{f}_\sigma$ is the surface tension force per unit volume concentrated on the interface (Γ), δ_Γ is the Dirac delta function concentrated at Γ. Physical properties (β) are defined as follows:

$$\beta = \beta_c H_c + \beta_d H_d, \;\; \beta = \{\rho, \mu, ...\} \tag{3}$$

H_c denotes the Heaviside step function, equal to one at Ω_c and zero elsewhere. $H_d = 1 - H_c$. Subscripts d and c denote the continuous phase (Ω_d) and dispersed phase (Ω_c), respectively. For cases with periodic boundary conditions in the vertical direction (parallel to $\mathbf{g}$), ρ_0 is defined as $\rho_0 = V_\Omega^{-1} \int_\Omega (\rho_d H_d + \rho_c H_c)\, dV$ [13, 6, 8, 21]. Otherwise, $\rho_0 = 0$.

2.2 Multi-marker UCLS method

The unstructured conservative level-set (UCLS) method proposed by Balcazar et al.[13, 7] performs interface capturing on three-dimensional unstructured meshes. On the other hand, the multiple marker UCLS approach introduced in Balcazar et al.[13, 4, 6, 8, 11] circumvents the numerical coalescence of fluid particles. In this framework, each marker is a level-set function [13, 11, 7], $\phi_i = 0.5\,(\tanh\,(d_i/(2\varepsilon)) + 1)$, where d_i is a signed distance function [48, 58]. Furthermore, ε is a parameter that sets the interface

thickness, i.e., at the cell Ω_P, $\varepsilon_P = 0.5(h_P)^\alpha$, $\alpha = 0.9$ unless otherwise stated, h_P is the local grid size [13, 11, 7, 21]. The ith interface advection equation is solved in conservative form:

$$\frac{\partial \phi_i}{\partial t} + \nabla \cdot (\phi_i \mathbf{v}) = 0,\ i = \{1, 2, ..., N_m\}. \tag{4}$$

where N_m denotes the number of level-set markers, here equivalent to the number of fluid particles $N_m = N_d$. The following unstructured re-initialization equation [13, 11, 7, 21] is solved to maintain a constant interface thickness:

$$\frac{\partial \phi_i}{\partial \tau} + \nabla \cdot \left(\phi_i(1-\phi_i)\mathbf{n}_i^0\right) = \nabla \cdot \left(\varepsilon \nabla \phi_i\right),\ i = \{1, 2, ..., N_m\}. \tag{5}$$

Eq.(5) is advanced in pseudo-time τ up to the steady-state, $\mathbf{n}_i^0$ is the interface normal unit vector at $\tau = 0$. Interface normal vectors ($\mathbf{n}_i$) and curvatures κ_i, are calculated as $\mathbf{n}_i = \nabla\phi_i / ||\nabla\phi_i||$, $\kappa_i = -\nabla \cdot \mathbf{n}_i$ [13, 8, 7, 21].

2.3 Energy equation

For thermocapillary migration of droplets, the temperature field ($T(\mathbf{x}, t)$) evolves according to the following energy transport equation [11]:

$$\rho c_p \left(\frac{\partial T}{\partial t} + \nabla \cdot (\mathbf{v}T) \right) = \nabla \cdot (\lambda \nabla T), \tag{6}$$

where $c_p = c_{p,d}H_d + c_{p,c}H_c$ is the specific heat capacity, and $\lambda = \lambda_d H_d + \lambda_c H_c$ is the thermal conductivity.

2.4 Surface tension and regularization of physical properties

Surface tension force ($\mathbf{f}_\sigma$, Eq.(1)) is calculated with the Continuous Surface Force (CSF) model [24], extended to the multi-marker UCLS method [8, 11, 6, 13, 15]:

$$\mathbf{f}_\sigma = \sum_{i=1}^{N_m} (\mathbf{f}_{\sigma,i}^{(n)} + \mathbf{f}_{\sigma,i}^{(t)}),\ \mathbf{f}_{\sigma,i}^{(n)} = \sigma\kappa_i \nabla\phi_i,\ \mathbf{f}_{\sigma,i}^{(t)} = (\nabla\sigma - \mathbf{n}_i(\mathbf{n}_i \cdot \nabla\sigma))||\nabla\phi_i||, \tag{7}$$

where $\mathbf{f}_{\sigma,i}^{(n)}$ is the normal component of the surface tension force, and $\mathbf{f}_{\sigma,i}^{(t)}$ is tangential to the interface, i.e., the so-called Marangoni force [30]. Furthermore, without surfactants, $\sigma = \sigma(T)$ is the surface tension coefficient with T defined as the temperature. A linear equation of state $\sigma = \sigma_0 + \sigma_T(T - T_0)$, $\sigma_0 = \sigma(T_0) > 0$ and $\sigma_T < 0$, is used unless otherwise stated.

Here, $\delta_{\Gamma,i}^s = ||\nabla\phi_i||$ is the regularized Dirac delta function concentrated at the interface [21, 15, 13, 7, 6]. Concerning the regularization of physical properties, H_c and H_d (Eq. (3)), are regularized by a global level-set function $\phi = \min\{\phi_1, ..., \phi_{n_d}\}$ [8, 21, 15, 13], e.g., $H_d^s = 1 - \phi$ and $H_c^s = \phi$ if $0 < \phi \leq 0.5$ for Ω_d, and $0.5 < \phi \leq 1$ for Ω_c. Alternatively, if $0 < \phi \leq 0.5$ for Ω_c, and $0.5 < \phi \leq 1$ for Ω_d, then $H_d = \phi$ and $H_c = 1 - \phi$, whereas $\phi = \max\{\phi_1, ..., \phi_{n_d}\}$ [13, 8, 7, 21]. For thermocapillary migration of droplets, physical properties are regularized as proposed in [11].

Transport equation	Convective term	β	ψ
Eq.(1)	$\nabla \cdot (\rho v_i \, \mathbf{v})$	ρ	v_i
Eq.(4)	$\nabla \cdot (\phi \, \mathbf{v})$	1	ϕ
Eq.(6)	$\nabla \cdot (T \, \mathbf{v})$	1	T

Table 1: Convective term of transport equations, v_i refers to the Cartesian components of $\mathbf{v}$.

2.5 Numerical methods

The finite-volume method is used for discretization of transport equations on 3D collocated unstructured meshes [13, 7, 21]. The convective term (Table 1) is explicitly computed by approximating the fluxes at cell faces with unstructured flux-limiter schemes, proposed by Balcazar et al.[13, 7, 20]. Indeed, a general approximation of the convective term in the cell Ω_P is written as follows:

$$(\nabla \cdot \beta\psi\mathbf{v})_P = V_P^{-1} \sum_f \beta_f \psi_f (\mathbf{v}_f \cdot \mathbf{A}_f), \tag{8}$$

where V_P is the volume of Ω_P, sub-index f denotes the cell-faces, $\mathbf{A}_f = ||\mathbf{A}_f|| \mathbf{e}_f$ is the area vector, $\mathbf{e}_f$ is a unit vector perpendicular to the face f pointing outside the cell Ω_P. Furthermore, $\psi_f = \psi_{C_p} + 0.5L(\theta_f)(\psi_{D_p} - \psi_{C_p})$, where $L(\theta_f)$ is the flux-limiter function, $\theta_f = (\psi_{C_p} - \psi_{U_p})/(\psi_{D_p} - \psi_{C_p})$, sub-index C_p denotes the upwind point, sub-index U_p refers to the far-upwind point, and sub-index D_p refers to the downwind point, as proposed in the framework of the UCLS method [13]. Table 1 outlines the definitions of β and ψ. Some of the flux-limiter functions [59, 33, 35, 41, 38] implemented on the unstructured multiphase solver [21, 15, 13, 7, 6] are summarized as follows:

$$L(\theta_f) \equiv \begin{cases} \max\{0, \min\{2\theta_f, 1\}, \min\{2, \theta_f\}\} & \text{SUPERBEE}, \\ \max\{0, \min\{2\theta_f, (2/3)\,\theta_f + (1/3), 2\}\} & \text{KOREN}, \\ \max\{0, \min\{4\theta_f, 0.75 + 0.25\theta_f, 2\}\} & \text{SMART}, \\ (\theta_f + |\theta_f|)/(1 + |\theta_f|) & \text{VANLEER}, \\ \text{minmod}\{1, \theta_f\} & \text{MINMOD}, \\ 0 & \text{UPWIND}, \\ 1 & \text{CD}. \end{cases} \tag{9}$$

The SUPERBEE flux-limiter funtion is used unless otherwise stated. On the other hand, the compressive term of the unstructured re-initialization equation (Eq. (5)) [7, 21, 13, 8], is discretized at the cell Ω_P as follows [21, 13]: $(\nabla \cdot \phi_i(1-\phi_i)\mathbf{n}_i^0)_P = \frac{1}{V_P} \sum_f (\phi_i(1-\phi_i))_f \mathbf{n}_{i,f}^0 \cdot \mathbf{A}_f$, where $\mathbf{n}_{i,f}^0$ and $(\phi_i(1-\phi_i))_f$ are linearly interpolated. The diffusive term of transport equations are centrally differenced [13]. Gradients are computed at cell centroids through the weighted least-squares method [21, 13, 16, 12, 7]. The fractional-step projection method [26, 49, 63] solves the pressure-velocity coupling in the momentum transport equation (Eq.(1)). Furthermore, the convective velocity $\mathbf{v}_f$ (Eq.(8)) is interpolated [11, 13] to avoid the so-called pressure-velocity decoupling on collocated meshes [51]. Then, the volume flux $(\mathbf{v}_f \cdot \mathbf{A}_f)$, normal velocity $(\mathbf{v}_f \cdot \mathbf{e}_f)$ [11]. The reader is referred to [13, 12, 16] for further technical details about the discretization of transport equations and examples of global algorithms.

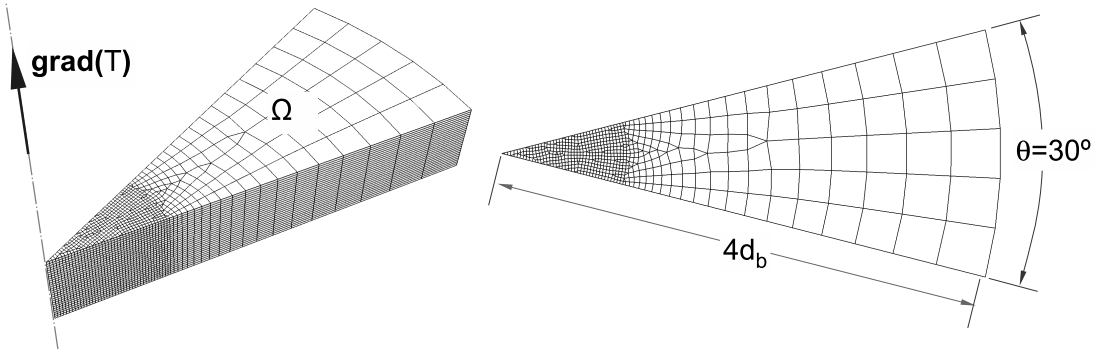

Figure 1: Example of mesh distribution for thermocapillary migration of a droplet on a fixed mesh. Ω is a section of a cylindrical domain, with angle $\theta = 30^{\circ}$, radius $R = 4\,d_b$ and height $L_y = 8\,d_b$ (parallel to **grad**(T)). Here, d_b is the spherical equivalent bubble or droplet diameter. Ω is discretized by hexahedrals and triangular prisms.

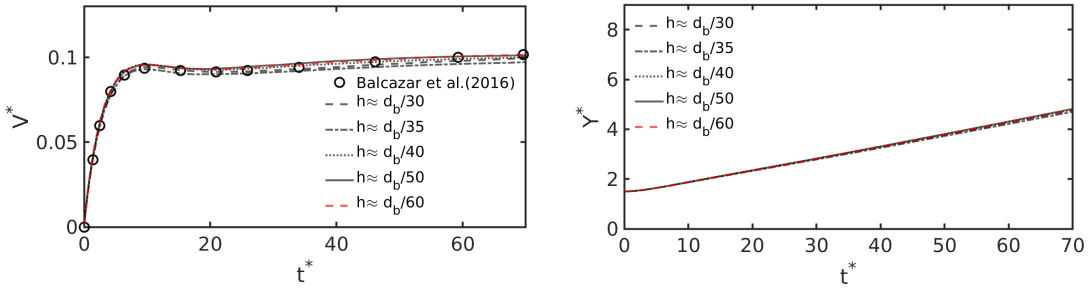

Figure 2: Thermocapillary migration of a droplet: $\mathbf{g} = \mathbf{0}$. $\mathrm{Re} = 20.0$, $\mathrm{Ma} = 50.0$, $\mathrm{Ca} = 0.041666$, $\eta_\rho = \rho_c/\rho_d = 1.0$, $\eta_\mu = \mu_c/\mu_d = 1.0$, $\eta_\lambda = \lambda_c/\lambda_d = 1.0$, $\eta_{c_p} = c_{p,c}/c_{p,d} = 1.0$. Dimensionless migration velocity $V^* = (\mathbf{e}_y \cdot \mathbf{v}_{c,i})/U_r$, $\mathbf{v}_{c,i}$ is the droplet velocity. Dimensionless time $t^* = t/t_r$. Dimensionless vertical position, $Y^* = (\mathbf{e}_y \cdot \mathbf{x}_{c,i})/d_b$, $\mathbf{x}_{c,i}$ is the droplet centroid. Symbols denote the reference results in a full three-dimensional cylindrical domain reported by Balcazar et al.(2016) [11].

3 NUMERICAL EXPERIMENTS

3.1 Validations and verifications

Verifications, validations and extensions of the unstructured multiphase flow solver [7, 9, 6, 13, 12] for interfacial transport processes include buoyancy-driven bubbles [7, 8, 6, 2], thermocapillary migration of droplets [11, 15], bubbly flows [10, 6, 13, 14, 16], falling droplets [5], binary droplet collision with bouncing outcome [10], bouncing collision of a droplet against a fluid-fluid interface [10], interfacial mass transfer in bubbly flows [16, 4, 13, 14], and liquid-vapor phase change [12, 18].

3.2 Thermocapillary migration of a droplet: Fixed unstructured collocated meshes

Thermocapillary migration of droplets is characterized by the physical properties ratios $\eta_\beta = \beta_c\,\beta_d^{-1}$, with $\beta = \{\rho, \mu, \lambda, c_p\}$, Capillary number $\mathrm{Ca} = (|\sigma_T|\,||\nabla T_\infty||\,d_b)\,(2\sigma_0)^{-1}$, Reynolds number $\mathrm{Re} = (|\sigma_T|\,||\nabla T_\infty||\,d_b^2\rho_c)\,(4\mu_c^2)^{-1}$, and Marangoni number $\mathrm{Ma} = (|\sigma_T|\,||\nabla T_\infty||\,d_b^2\rho_c c_{p,c})\,(4\mu_c\lambda_c)^{-1}$, sub-index c denotes the continuous phase and sub-index d denotes the dispersed phase (droplet), d_b is the

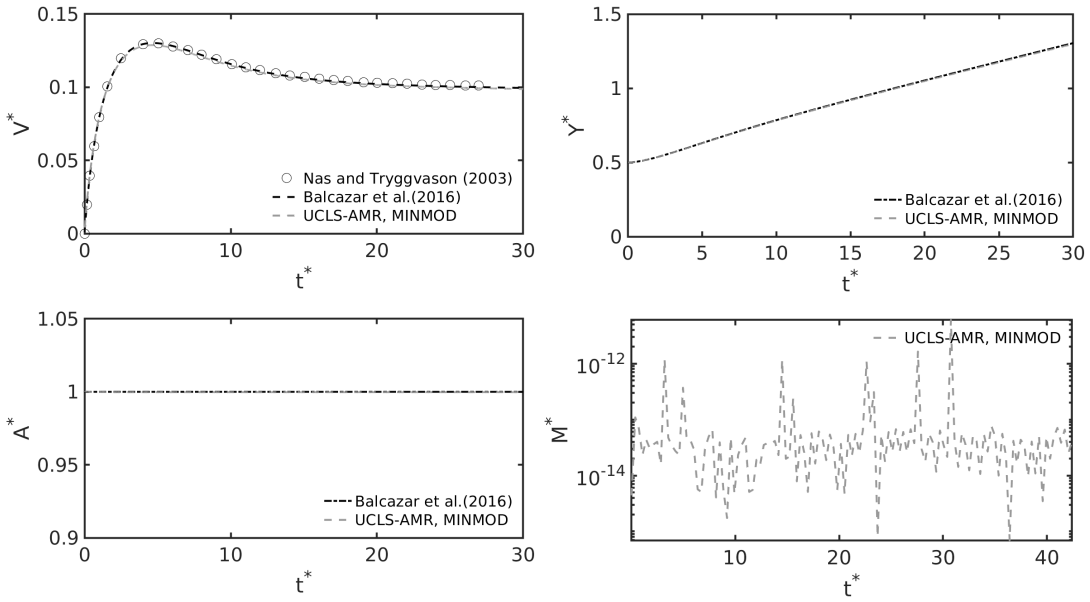

Figure 3: Thermocapillary migration of a single droplet using adaptive mesh refinement (AMR) on a collocated unstructured mesh, and MINMOD flux-limiter convective scheme (Eq.(9)). Here, $\mathbf{g} = \mathbf{0}$, $\mathrm{Ca} = 0.01666$, $\mathrm{Re} = 5.0$, $\mathrm{Ma} = 20.0$, $\eta_\rho = \rho_c/\rho_d = 2.0$, $\eta_\mu = \mu_c/\mu_d = 2.0$, $\eta_\lambda = \lambda_c/\lambda_d = 2.0$, $\eta_{c_p} = c_{p,c}/c_{p,d} = 2.0$. Present UCLS and AMR simulations against front tracking simulations of Nas and Tryggvason (2003) [45], and UCLS simulation on a fixed mesh of Balcazar et al.(2016) [11]. Here, $t^* = t/t_r$. (a) Migration velocity $V^* = (\mathbf{e}_y \cdot \mathbf{v})U_r^{-1}$. (b) Dimensionless droplet surface $A^* = A(t)/A(0)$, $A(t) = \int_\Omega ||\nabla\phi|| dV$. (c) Dimensionless position of the droplet on the y-axis, $Y^* = y/L_x$. (d) Mass conservation error $M^* = |(M(t) - M(0))/M(0)|$, $M(t) = \int_\Omega H_d^s dV$.

spherical equivalent bubble or droplet diameter, $\nabla T_\infty = ((T_h - T_c)/L_y)\mathbf{e}_y$, T_h is the temperature at the top boundary (hot), and T_c is the temperature at the bottom boundary (cold). Furthermore, the reference velocity $U_r = |\sigma_T|\,||\nabla T_\infty||(0.5d_b)/\mu_c$, reference temperature $T_r = ||\nabla T_\infty||(0.5d)$, and reference time $t_r = 0.5d/U_r$, are defined to report the numerical results.

Figure 1 illustrates the computational setup for simulating single droplets within an axial-symmetric domain. The domain (Ω) is discretized with hexahedral volumes and triangular prisms, with a grid resolution equivalent to solving the droplets with $h = h_{\min} \approx \{d_b/30, d_b/35, d_b/40, d_b/50, d_b/60\}$ around the symmetry axis of Ω, using 118440 up to 521280 control volumes, distributed in 16 up to 48 CPU-cores, respectively. Neumann boundary conditions are applied to $\{\phi, T\}$ in all boundaries. Concerning the velocity field $\mathbf{v}$, non-slip boundary conditions are applied to the cylinder wall and top and bottom boundaries, whereas the Neumann boundary condition applies to the angular boundaries. The initial position of the bubble is set on the symmetry axis at a distance of $1.5\,d_b$ from the bottom boundary, with the surrounding fluids initially at rest. The initial temperature field follows a linear distribution from the bottom boundary up to the top boundary.

The dimensionless parameters are $\mathrm{Re} = 20.0$, $\mathrm{Ma} = 50.0$, $\mathrm{Ca} = 0.041666$, $\eta_\rho = \rho_c/\rho_d = 1.0$, $\eta_\mu = \mu_c/\mu_d = 1.0$, $\eta_\lambda = \lambda_c/\lambda_d = 1.0$, and $\eta_{c_p} = c_{p,c}/c_{p,d} = 1.0$. Furthermore, $\mathbf{g} = \mathbf{0}$. Figures 2 show the dimensionless migration velocity and the dimensionless position of the droplet. The present axial-symmetrical simulations are in close agreement with UCLS simulations [11] performed on a tree-dimensional cylinder, proving the capability of the UCLS method to solve two-phase flows with

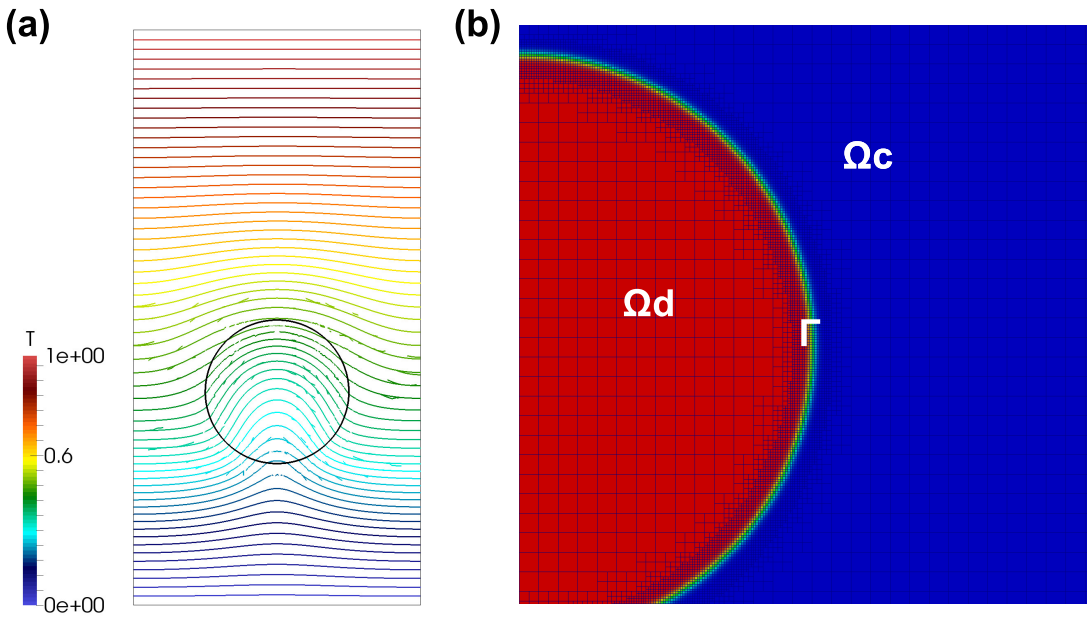

Figure 4: Thermocapillary migration of a single droplet using UCLS and AMR, $\mathbf{g} = \mathbf{0}$. (a) Temperature isocontours. (b) Adaptive mesh refinement (AMR) around the interface (Γ). The maximum grid size is $h_{max} = L_x/60$, and the minimum grid size is $h_{min} = h_{max}/2^4$.

interfacial heat transfer and Marangoni stresses on fixed unstructured meshes with non-orthogonal and mixed control volumes.

3.3 Thermocapillary migration of a droplet: hexahedral Adaptive Mesh Refinement (AMR)

Reference results for this case were reported by [45] using the front-tracking method, [11] using the UCLS method on fixed hexahedral meshes, and [17, 15] using UCLS, hexahedral AMR and SUPERBEE, SMART, VANLEER, UPWIND flux-limiter convective schemes (Eq.(9)). Here, this case is solved using the UCLS-AMR framework and the MINMOD convective scheme (Eq.(9)). The hexahedral AMR technique was first reported for single-phase turbulent flows [3], and further extended and optimized to perform DNS of isothermal bubbles at high Reynolds numbers [2] in the framework of the UCLS method proposed by Balcazar et al.[13, 5, 7]. The computational setup consists of a rectangle domain (Ω) extending $L_x = 4d_b$ in the x direction and $L_y = 8d_b$ in the y direction. As an initial condition, the droplet centroid is located above the bottom wall at a distance d_b. Non-slip boundary conditions are applied on the top and bottom walls with fixed temperatures T_h and $T_c < T_h$, respectively. On the other hand, the periodic boundary condition is applied to lateral boundaries (x-axis). The material property ratios η_ρ, η_μ, η_{c_p} and η_λ are set to 0.5, whereas the dimensionless parameters are chosen as $\mathrm{Re} = 5$, $\mathrm{Ma} = 20$, and $\mathrm{Ca} = 0.016\bar{6}$. Figure 3 demonstrates that numerical results computed by the AMR-UCLS method and MINMOD flux-limiter convective scheme are consistent with reference results reported by [45] and [11] on fixed meshes, whereas mass conservation error is under control. Figure 3 illustrates an snapshot of the temperature field and details on the adaptive refinement around the interface.

4 CONCLUSIONS

The UCLS method for two-phase flow with interfacial heat and mass transfer on fixed and adaptive collocated unstructured meshes has been introduced. The capabilities of the unstructured multiphase solver have been proven for thermocapillary migration of droplets using AMR and fixed meshes. An appropriate selection of the unstructured flux-limiters schemes proposed by Balcazar et al.[13, 7], to discretize the convective term of transport equations, minimize the so-called numerical diffusion and circumvents numerical oscillations around the interface. Numerical schemes have led to a robust and accurate numerical code for simulating two-phase flows with interfacial transport processes on collocated unstructured meshes with mixed control volumes on fixed meshes, and hexahedral AMR. Ongoing work includes extensions of the UCLS method to nucleate boiling, and simultaneous heat and mass transfer.

ACKNOWLEDGMENTS

The principal author, N. Balcázar-Arciniega, as Serra-Hunter Lecturer (UPC-LE8027), acknowledges the financial support provided by the Catalan Government through this program. Simulations were conducted using computing resources allocated by the RES under the project IM-2024-1-0007 on the supercomputer MareNostrum V, at the BSC, Barcelona, Spain. The authors acknowledge the financial support of the MCIN/AEI/10.13039/501100011033 under the project PID2020-115837RB-100, Spain.

REFERENCES

[1] ABOULHASANZADEH, B., HOSODA, S., TOMIYAMA, A., AND TRYGGVASON, G. A validation of an embedded analytical description approach for the computations of high Schmidt number mass transfer from bubbles in liquids. *Chemical Engineering Science 101* (sep 2013), 165–174.

[2] ANTEPARA, O., BALCÁZAR, N., RIGOLA, J., AND OLIVA, A. Numerical study of rising bubbles with path instability using conservative level-set and adaptive mesh refinement. *Computers and Fluids 187* (2019), 83–97.

[3] ANTEPARA, O., LEHMKUHL, O., BORRELL, R., CHIVA, J., AND OLIVA, A. Parallel adaptive mesh refinement for large-eddy simulations of turbulent flows. *Computers and Fluids 110* (mar 2015), 48–61.

[4] BALCAZAR, N., ANTEPARA, O., RIGOLA, J., AND OLIVA, A. DNS of Drag-Force and Reactive Mass Transfer in Gravity-Driven Bubbly Flows. *In: García-Villalba, M., Kuerten, H., Salvetti, M. (eds) Direct and Large Eddy Simulation XII. DLES 2019. ERCOFTAC Series, vol 27. Springer, Cham* (2020), 119–125.

[5] BALCAZAR, N., CASTRO, J., CHIVA, J., AND OLIVA, A. DNS of falling droplets in a vertical channel. *International Journal of Computational Methods and Experimental Measurements 6*, 2 (nov 2017), 398–410.

[6] BALCAZAR, N., CASTRO, J., RIGOLA, J., AND OLIVA, A. DNS of the wall effect on the motion of bubble swarms. *Procedia Computer Science 108* (2017), 2008–2017.

[7] BALCÁZAR, N., JOFRE, L., LEHMKUHL, O., CASTRO, J., AND RIGOLA, J. A finite-volume/level-set method for simulating two-phase flows on unstructured grids. *International Journal of Multiphase Flow 64* (sep 2014), 55–72.

[8] BALCAZAR, N., LEHMKUHL, O., JOFRE, L., AND OLIVA, A. Level-set simulations of buoyancy-driven motion of single and multiple bubbles. *International Journal of Heat and Fluid Flow 56* (2015).

[9] BALCAZAR, N., LEHMKUHL, O., JOFRE, L., RIGOLA, J., AND OLIVA, A. A coupled volume-of-fluid/level-set method for simulation of two-phase flows on unstructured meshes. *Computers and Fluids 124* (2016), 12–29.

[10] BALCAZAR, N., LEHMKUHL, O., RIGOLA, J., AND OLIVA, A. A multiple marker level-set method for simulation of deformable fluid particles. *International Journal of Multiphase Flow 74* (2015), 125–142.

[11] BALCÁZAR, N., RIGOLA, J., CASTRO, J., AND OLIVA, A. A level-set model for thermocapillary motion of deformable fluid particles. *International Journal of Heat and Fluid Flow 62* (dec 2016), 324–343.

[12] BALCAZAR, N., RIGOLA, J., AND OLIVA, A. Unstructured Level-Set Method For Saturated Liquid-Vapor Phase Change. *In: WCCM-ECCOMAS 2020. Volume 600 - Fluid Dynamics and Transport Phenomena.* (2021), 1–12.

[13] BALCAZAR-ARCINIEGA, N., ANTEPARA, O., RIGOLA, J., AND OLIVA, A. A level-set model for mass transfer in bubbly flows. *International Journal of Heat and Mass Transfer 138* (2019), 335–356.

[14] BALCAZAR-ARCINIEGA, N., RIGOLA, J., AND OLIVA, A. DNS of Mass Transfer from Bubbles Rising in a Vertical Channel. *Lecture Notes in Computer Science (including subseries Lecture Notes in Artificial Intelligence and Lecture Notes in Bioinformatics) 11539 LNCS* (2019), 596–610.

[15] BALCAZAR-ARCINIEGA, N., RIGOLA, J., AND OLIVA, A. A level-set model for two-phase flow with variable surface tension: Thermocapillary and surfactants. *8th European Congress on Computational Methods in Applied Sciences and Engineering* (2022).

[16] BALCAZAR-ARCINIEGA, N., RIGOLA, J., AND OLIVA, A. DNS of mass transfer in bi-dispersed bubble swarms. *In: Computational Science – ICCS 2022. ICCS 2022. Lecture Notes in Computer Science, vol 13353. Springer, Cham 13353* (2022), 284–296.

[17] BALCÁZAR-ARCINIEGA, N., RIGOLA, J., AND OLIVA, A. DNS of Thermocapillary Migration of a Bi-dispersed Suspension of Droplets. *In: Computational Science – ICCS 2023. ICCS 2023. Lecture Notes in Computer Science*, 2016153612 (2023), 303–317.

[18] BALCAZAR-ARCINIEGA, N., RIGOLA, J., AND OLIVA, A. Unstructured Conservative Level-Set (UCLS) Simulations of Film Boiling Heat Transfer. *In: Computational Science – ICCS 2023. ICCS 2023. Lecture Notes in Computer Science 10477* (2023), 318–331.

[19] BALCAZAR-ARCINIEGA, N., RIGOLA, J., AND OLIVA, A. DNS of Mass Transfer in Bi-dispersed Bubbly Flows in a Vertical Pipe. In *ERCOFTAC Series*, vol. 31. 2024, pp. 55–61.

[20] BALCÁZAR-ARCINIEGA, N., RIGOLA, J., AND OLIVA, A. Unstructured Flux-Limiter Convective Schemes for Simulation of Transport Phenomena in Two-Phase Flows. *Lecture Notes in Computer Science, vol 14838. Springer, Cham.* (2024), 20–32.

[21] BALCÁZAR-ARCINIEGA, N., RIGOLA, J., PÉREZ-SEGARRA, C. D., AND OLIVA, A. Numerical study of the drag force, interfacial area and mass transfer in bubbles in a vertical pipe. *Chemical Engineering Journal 495* (sep 2024), 153124.

[22] BOTHE, D., AND FLECKENSTEIN, S. A Volume-of-Fluid-based method for mass transfer processes at fluid particles. *Chemical Engineering Science* (2013).

[23] BOTHE, D., KOEBE, M., WIELAGE, K., AND WARNECKE, H.-J. VOF-Simulations of Mass Transfer From Single Bubbles and Bubble Chains Rising in Aqueous Solutions. In *Volume 2: Symposia, Parts A, B, and C* (jan 2003), ASMEDC, pp. 423–429.

[24] BRACKBILL, J. U., KOTHE, D. B., AND ZEMACH, C. A continuum method for modeling surface tension. *Journal of Computational Physics 100*, 2 (1992), 335–354.

[25] BRADY, P. T., HERRMANN, M., AND LOPEZ, J. M. Confined thermocapillary motion of a three-dimensional deformable drop. *Physics of Fluids 23*, 2 (feb 2011), 022101.

[26] CHORIN, A. J. Numerical Solution of the Navier-Stokes Equations. *Mathematics of Computation 22*, 104 (1968), 745.

[27] CLIFT, R., GRACE, J., AND WEBER, M. *Bubbles, Drops, and Particles*. DOVER PUBLICATIONS, INC, New York, 1978.

[28] DARMANA, D., DEEN, N. G., AND KUIPERS, J. A. M. Detailed 3D Modeling of Mass Transfer Processes in Two-Phase Flows with Dynamic Interfaces. *Chemical Engineering Technology 29*, 9 (sep 2006), 1027–1033.

[29] DAVIDSON, M. R., AND RUDMAN, M. VOLUME-OF-FLUID CALCULATION OF HEAT OR MASS TRANSFER ACROSS DEFORMING INTERFACES IN TWO-FLUID FLOW. *Numerical Heat Transfer, Part B: Fundamentals 41*, 3-4 (mar 2002), 291–308.

[30] DEEN, W. *Analysis of Transport Phenomena*. OXFORD UNIV PR, 2011.

[31] ESMAEELI, A., AND TRYGGVASON, G. A front tracking method for computations of boiling in complex geometries. *International Journal of Multiphase Flow 30*, 7-8 (jul 2004), 1037–1050.

[32] ESMAEELI, A., AND TRYGGVASON, G. Computations of film boiling. Part I: numerical method. *International Journal of Heat and Mass Transfer 47*, 25 (2004), 5451–5461.

[33] GASKELL, P. H., AND LAU, A. K. C. Curvature-compensated convective transport: SMART, A new boundedness- preserving transport algorithm. *International Journal for Numerical Methods in Fluids 8*, 6 (1988), 617–641.

[34] GIBOU, F., FEDKIW, R. P., CHENG, L.-T., AND KANG, M. A Second-Order-Accurate Symmetric Discretization of the Poisson Equation on Irregular Domains. *Journal of Computational Physics 176*, 1 (feb 2002), 205–227.

[35] GUENTHER, C., AND SYAMLAL, M. The effect of numerical diffusion on simulation of isolated bubbles in a gas-solid fluidized bed. *Powder Technology* (2001).

[36] HIRT, C., AND NICHOLS, B. Volume of fluid (VOF) method for the dynamics of free boundaries. *Journal of Computational Physics 39*, 1 (jan 1981), 201–225.

[37] JURIC, D., AND TRYGGVASON, G. Computations of boiling flows. *International Journal of Multiphase Flow 24*, 3 (apr 1998), 387–410.

[38] KOREN, B. A Robust Upwind Discretization Method for Advection, Diffusion and Source Terms. *In: Numerical Methods for Advection-Diffusion Problems, C. Vreugdenhil and B. Koren, eds., vol. 45 of Notes on Numerical Fluid Mechanics, Vieweg, Braunschweig* (1993), 117–138.

[39] KOYNOV, A., KHINAST, J. G., AND TRYGGVASON, G. Mass transfer and chemical reactions in bubble swarms with dynamic interfaces. *AIChE Journal 51*, 10 (oct 2005), 2786–2800.

[40] KUMAR SINGH, N., AND PREMACHANDRAN, B. A coupled level set and volume of fluid method on unstructured grids for the direct numerical simulations of two-phase flows including phase change. *International Journal of Heat and Mass Transfer 122* (jul 2018), 182–203.

[41] LEVEQUE, R. J. *Finite Volume Methods for Hyperbolic Problems*. 2002.

[42] MA, C., AND BOTHE, D. Direct numerical simulation of thermocapillary flow based on the Volume of Fluid method. *International Journal of Multiphase Flow 37*, 9 (nov 2011), 1045–1058.

[43] MA, C., AND BOTHE, D. Numerical modeling of thermocapillary two-phase flows with evaporation using a two-scalar approach for heat transfer. *Journal of Computational Physics 233* (jan 2013), 552–573.

[44] NAS, S., MURADOGLU, M., AND TRYGGVASON, G. Pattern formation of drops in thermocapillary migration. *International Journal of Heat and Mass Transfer 49*, 13-14 (jul 2006), 2265–2276.

[45] NAS, S., AND TRYGGVASON, G. Thermocapillary interaction of two bubbles or drops. *International Journal of Multiphase Flow 29*, 7 (jul 2003), 1117–1135.

[46] NINGEGOWDA, B., AND PREMACHANDRAN, B. A Coupled Level Set and Volume of Fluid method with multi-directional advection algorithms for two-phase flows with and without phase change. *International Journal of Heat and Mass Transfer 79* (dec 2014), 532–550.

[47] OLSSON, E., AND KREISS, G. A conservative level set method for two phase flow. *Journal of Computational Physics 210*, 1 (nov 2005), 225–246.

[48] OSHER, S., AND SETHIAN, J. A. Fronts propagating with curvature-dependent speed: Algorithms based on Hamilton-Jacobi formulations. *Journal of Computational Physics 79*, 1 (nov 1988), 12–49.

[49] PROSPERETTI, A., AND TRYGGVASON, G. *Computational Methods for Multiphase Flow*. Cambridge University Press, Cambridge, 2007.

[50] RAJKOTWALA, A., PANDA, A., PETERS, E., BALTUSSEN, M., VAN DER GELD, C., KUERTEN, J., AND KUIPERS, J. A critical comparison of smooth and sharp interface methods for phase transition. *International Journal of Multiphase Flow 120* (nov 2019), 103093.

[51] RHIE, C. M., AND CHOW, W. L. Numerical study of the turbulent flow past an airfoil with trailing edge separation. *AIAA Journal 21*, 11 (1983), 1525–1532.

[52] ROGHAIR, I., VAN SINT ANNALAND, M., AND KUIPERS, J. An improved Front-Tracking technique for the simulation of mass transfer in dense bubbly flows. *Chemical Engineering Science 152* (oct 2016), 351–369.

[53] SATO, Y., AND NIČENO, B. A sharp-interface phase change model for a mass-conservative interface tracking method. *Journal of Computational Physics 249* (sep 2013), 127–161.

[54] SON, G., AND DHIR, V. K. Numerical Simulation of Film Boiling Near Critical Pressures With a Level Set Method, feb 1998.

[55] SUN, D., AND TAO, W. A coupled volume-of-fluid and level set (VOSET) method for computing incompressible two-phase flows. *International Journal of Heat and Mass Transfer 53*, 4 (jan 2010), 645–655.

[56] SUSSMAN, M., AND PUCKETT, E. G. A Coupled Level Set and Volume-of-Fluid Method for Computing 3D and Axisymmetric Incompressible Two-Phase Flows. *Journal of Computational Physics 162*, 2 (aug 2000), 301–337.

[57] SUSSMAN, M., SMEREKA, P., AND OSHER, S. A Level Set Approach for Computing Solutions to Incompressible Two-Phase Flow. *Journal of Computational Physics 114*, 1 (sep 1994), 146–159.

[58] SUSSMAN, M., SMEREKA, P., AND OSHER, S. A Level Set Approach for Computing Solutions to Incompressible Two-Phase Flow. *Journal of Computational Physics 114*, 1 (sep 1994), 146–159.

[59] SWEBY, P. K. High Resolution Schemes Using Flux Limiters for Hyperbolic Conservation Laws. *SIAM Journal on Numerical Analysis 21*, 5 (oct 1984), 995–1011.

[60] TANGUY, S., MÉNARD, T., AND BERLEMONT, A. A Level Set Method for vaporizing two-phase flows. *Journal of Computational Physics 221*, 2 (feb 2007), 837–853.

[61] TOMAR, G., BISWAS, G., SHARMA, A., AND WELCH, S. W. J. Multimode analysis of bubble growth in saturated film boiling. *Physics of Fluids 20*, 9 (sep 2008), 092101.

[62] TRYGGVASON, G., BUNNER, B., ESMAEELI, A., JURIC, D., AL-RAWAHI, N., TAUBER, W., HAN, J., NAS, S., AND JAN, Y.-J. A Front-Tracking Method for the Computations of Multiphase Flow. *Journal of Computational Physics 169*, 2 (may 2001), 708–759.

[63] TRYGGVASON, G., SCARDOVELLI, R., AND ZALESKI, S. *Direct numerical simulations of Gas-Liquid multiphase flows*. 2011.

[64] WELCH, S. W., AND WILSON, J. A Volume of Fluid Based Method for Fluid Flows with Phase Change. *Journal of Computational Physics 160*, 2 (may 2000), 662–682.

[65] YUAN, M., YANG, Y., LI, T., AND HU, Z. Numerical simulation of film boiling on a sphere with a volume of fluid interface tracking method. *International Journal of Heat and Mass Transfer 51*, 7-8 (apr 2008), 1646–1657.